J Sol-Gel Sci Techn (2006) 37: 189–193
DOI 10.1007/s10971-005-6627-9

ORIGINAL ARTICLE

Amorphous sol-gel titania modified with heteropolyacids

T. López · E. Ortiz · R. Gómez · M. Picquart

Published online: 24 February 2006

Abstract Samples of amorphous sol-gel titania were prepared at 50%wt with tungstophosphoric or molybdophosphoric acid. The resulting gels were dried and annealed at 100, 150 and 200°C and studied by FT-IR, UV-Vis, EPR, TGA and Raman spectroscopy. By FT-IR the evolution of the stretching vibration of the OH groups (3450–3700 cm^{-1}) was followed. The intensity of this band decreased as the annealing temperature increased. With UV-Vis spectroscopy the band gap was determined for each sample, and the Eg was found between 2.72 and 3.38 eV. Raman spectroscopy revealed the formation of Mo—O—Ti and W—O—Ti—O bonds. An intense EPR signal at $g = 1.998$ was observed during annealing of the samples. Amorphous solids with a significant number of vacancies and promising photocatalytic properties were obtained.

1. Introduction

Photocatalysis by TiO_2 semiconductors has received much attention and been widely studied, with the final aim of an efficient conversion of solar energy into useful chemical energy [1]. TiO_2 semiconductors are ideal photocatalysts due to their chemical stability, low toxicity, and high photocalytic reactivity in the elimination of pollutants in air and water. TiO_2 semiconductor photocatalysts can oxidize a wide range of organic compounds, such as dioxins [2], phenols [3], cresols [4], alcohols [5], surfactants and dyes into harmless compounds such as CO_2 and H_2O by irradiation with UV light [6]. Illumination of such photocatalysts with light energy greater than the semiconductor band gap ($h\nu > E_g$) produces electron—hole pairs of high energy that can migrate to the material's surface and initiate redox reactions, which can lead to complete mineralization of the organic pollutants.

A suitable band gap is essential for catalytic efficiency. Doped TiO_2 samples have band gaps falling in the 2.91–3.2 eV range but this is not the sole criterion. Other factors may have a great influence. These include surface area, catalyst morphology, adsorption capacity and even particle size.

It has been reported that transition metals supported on TiO_2 play the role of electron traps, thus improving the oxidation process since the recombination of holes and electrons induced by UV irradiation is avoided [7]. The photoefficiency depends on both the energy of the band gap and the electron-hole pair recombination. Recent studies have shown that SO_4^{2-} ions anchored on the surface appear to play a similar role [8].

Heteropoly acids (HPAs), particularly $H_3PW_{12}O_{40}$, have been employed to modify the TiO_2 particle surface. They have received significant attention as reagents or catalysts for redox processes involving organic substrates, since it is well known that they are good electron acceptor that can store several electrons per molecule [9]. $H_3PW_{12}O_{40}$ has also been reduced in the presence of alcohol upon illumination with near-UV light, producing heteropoly blue [10]. The blues are known to be moderate reducing agents that can sensitize the photochemical reduction of oxygen and water [11]. Thus, HPAs incorporated into TiO_2 could

T. López (✉) · E. Ortiz · R. Gómez
Departamento de Química, Universidad Autónoma Metropolitana- Iztapalapa,
Apdo. postal 55-534, 09340 México, D.F., México
e-mail: tesy@xanum.uam.mx

M. Picquart
Departamento de Física, Universidad Autónoma Metropolitana-Iztapalapa Apdo. postal 55-534 09340 México, D.F., México

be useful photosystems for the photodegradation of organic contaminants in water [12].

In the present work, the sol-gel process was used to incorporate HPAs as tungstophosphoric acid (HWP) and molybdophosphoric acid (HMoP) into titania prepared from titanium n-butoxide hydrolysis. The materials obtained were characterized by FTIR, Raman spectroscopy, UV-Vis spectroscopy, EPR and TGA analysis.

2. Experimental methods

2.1. Sample preparation

Titania sol-gel catalysts with 50% w/w of HWP or HMoP, here referred to as Ti-HWP-50 or Ti-HMoP-50, respectively, were prepared as follow: In a glass reflux system were added 175 ml of water and 175 ml of tert-butanol. Then, the pH was adjusted to pH 3 with concentrated HNO_3 and the temperature was maintained at 70°C. Afterwards, HWP or HMoP were dissolved in a mixture of 25 ml of water and 25 ml of tert-butanol, and the resulting solution was added drop-wise to the reflux system with the simultaneous addition of 75 ml of titanium n-butoxide over 4 h. After gelation (24 h at 70°C), the samples were treated thermally at 100, 150 and 200 °C for 4 h. The heating rate was 2°C/min.

2.2. FTIR-spectroscopy

Infrared spectroscopy was performed using a PERKIN ELMER Paragon 2000 spectrophotometer. The samples were diluted in KBr (10% sample and 90% KBr) and were pressed into thin wafers for study.

2.3. Raman scattering

The Raman scattering experiments were performed at room temperature on a computerized Spex 1403 double monochromator, using a Lexel Ar^+ laser. The 514.5 nm laser line was used, with a power of 40 mW at the laser head and the spectral resolution was about 2 cm^{-1}. The scattered light, detected in a backscattering geometry, was collected on the photocathode of a cooled photomultiplier interfaced to a standard photon counting system.

2.4. UV-vis absorption

The UV-VIS absorption spectra were obtained using a Cary III spectrophotometer equipped with an integrating sphere for diffuse reflectance studies. MgO (100%) was used as a reflectance reference.

2.5. EPR

Electron paramagnetic resonance measurements were performed on a JEOL JES-RE3X spectrometer, using a cylindrical cavity (TE_{011} mode) with a 100 kHz field modulation. g values were obtained by measuring the resonance field with a JEOL ES-FC5 NMR gauss meter, while the operating frequency was measured with a HP-5350B counter.

2.6. TGA

Thermogravimetric analyses were performed on a Shimadzu DT-30 analyzer. Fresh samples were placed in a cell and heated in flowing nitrogen at 10°C/min.

3. Experimental results

3.1. FT-IR absorption

The FTIR spectra of Ti–HWP-50 as a function of annealing temperature from 70°C (fresh sample) to 200°C are shown in Fig. 1. In the fresh sample, the FT-IR spectrum is characterized by a very strong and broad absorption band centered near 610 cm^{-1} with shoulders at 339, 461, 679, 813, 897

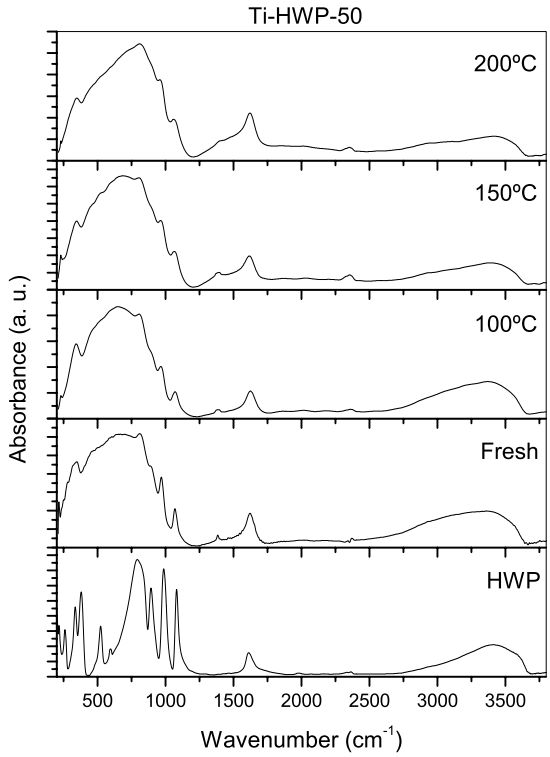

Fig. 1 FTIR absorption spectra of Ti-HWP-50 (measured at room temperature) as a function of annealing temperature. The spectrum of pure HWP acid is shown in the bottom trace.

and 969 cm^{-1}. Three bands can also be seen at 1069, 1386 and 1630 cm^{-1}, together with a broad band near 3350 cm^{-1}. Absorptions at 264, 337, 381, 525, 596, 796, 895, 989 and 1082 cm^{-1} are observed in the FTIR spectrum of the pure acid (Fig. 1, bottom spectrum) in agreement with the results obtained by Rocchiccioli-Deltcheff *et al.*[13]. The four absorptions at 796, 895, 989 and 1082 cm^{-1} are characteristic of the Keggin anion; the first three are attributed to W-O-W stretches and the last to a P-O stretch [14].

The low wavenumber absorptions are assigned to ν_{Ti-O} (610 cm^{-1}) and $\delta_{Ti-O-Ti}$ (461 cm^{-1}), respectively [15]. The band at 1386 cm^{-1} is presumably due to residual titanium n-butoxide used in the sample synthesis. The 1630 cm^{-1} band is assigned to the δ_{OH} bending mode of adsorbed water, while the peak at 3350 cm^{-1} is attributed to ν_{O-H} stretching modes of water occluded in the titania network, residual alcohol and to hydroxyl groups (Ti–OH) [16]. All bands which involve vibrations of oxygen atoms (ν_{Ti-O}, $\delta_{Ti-O-Ti}$, ν_{O-H}-δ_{O-H}) of the matrix are still observed in the annealed samples but with a reduced intensity due to the desorption of hydroxyl species during heating. Shoulders due to the Keggin structure are also observed in the annealed samples.

Similar spectra are observed for Ti-HMoP-50 (Fig. 2) but with some small low-wavenumber shifts arising from the replacement of tungsten atoms with molybdenum atoms. In particular, the bands due to the Keggin structure are encountered at 791, 870, 969 and 1066 cm^{-1} in HMoP and at 805, 963 and 1065 cm^{-1} in Ti-HMoP-50.

3.2. Raman spectroscopy

In Fig. 3 the Raman spectrum of Ti–HWP-50 is compared to the spectrum of pure HWP acid. The latter spectrum is characterized by bands at 989 and 1012 cm^{-1}, which are assigned to antisymmetric and symmetric stretching modes of W-O octahedra, respectively [13]. Both are the signatures of the Keggin structure and are in agreement with previous results [13].

In the annealed samples, a weak, poorly resolved band can be observed near 996 cm^{-1}, showing that the Keggin structure is retained. Bands at 152, 400, 514 and 635 cm^{-1} that are characteristics of the anatase phase of TiO_2 are also observed [17]. However, the relatively large bandwidth (~30 cm^{-1}) suggests that the samples are a mixture of amorphous TiO_2 and anatase. The spectrum of Ti-HMoP-50 (Fig. 4) shows similar characteristics but with the band due to the Keggin structure at 995 cm^{-1} in the pure acid and near 965 cm^{-1} in the Ti−HMoP-50 material, respectively.

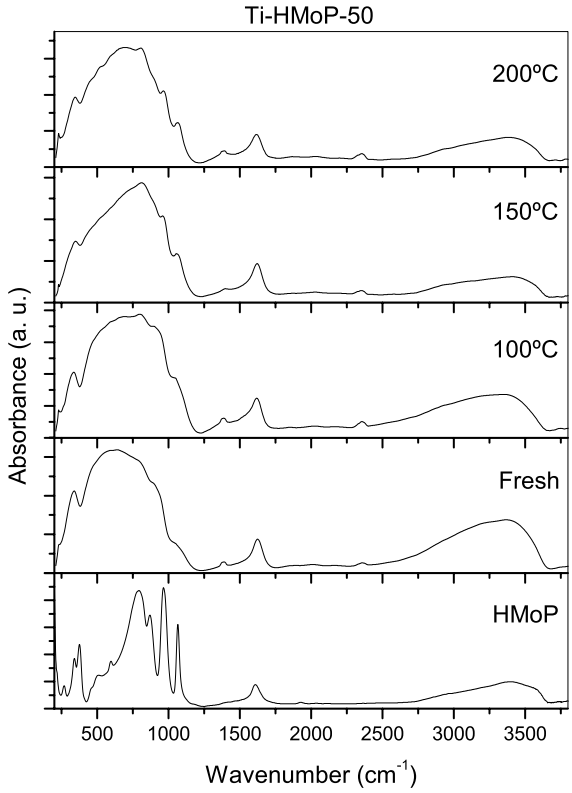

Fig. 2 FTIR absorption spectra of Ti-HMoP-50 (measured at room temperature) as a function of annealing temperature. The spectrum of pure HMoP acid is shown in the bottom trace.

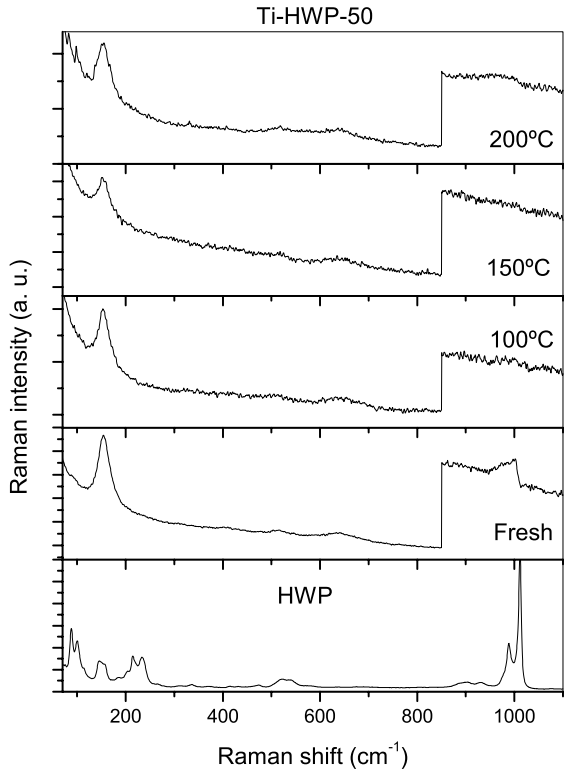

Fig. 3 Raman spectra of Ti-HWP-50 (measured at room temperature) as a function of annealing temperature. The spectrum of pure HWP acid is shown in the bottom trace.

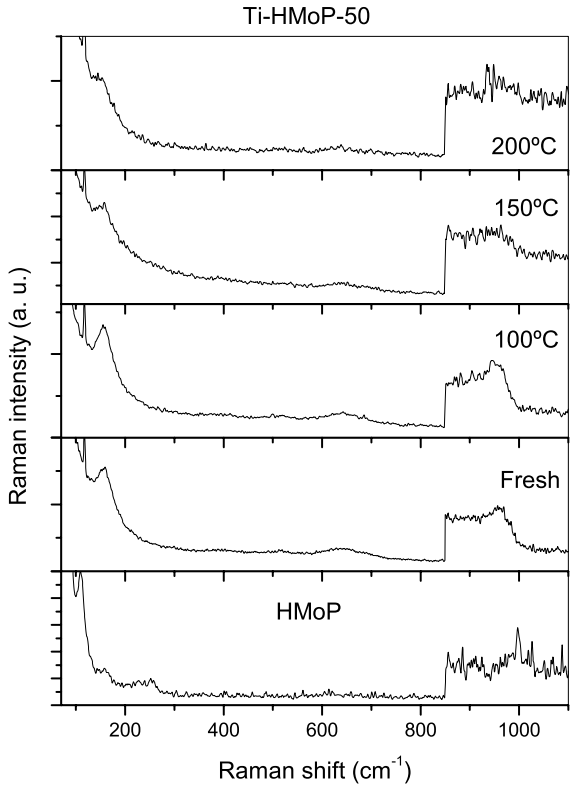

Fig. 4 Raman spectra of Ti-HMoP-50 (measured at room temperature) as a function of annealing temperature. The spectrum of pure HMoP acid is shown in the bottom trace.

3.3. UV-Vis absorption

The UV-Vis spectrum of each sample was obtained as a function of the annealing temperature. As an example, the behavior of Ti–HMoP-50 is presented in Fig. 5 as a function of the annealing temperature. The band gap was determined from the following equation:

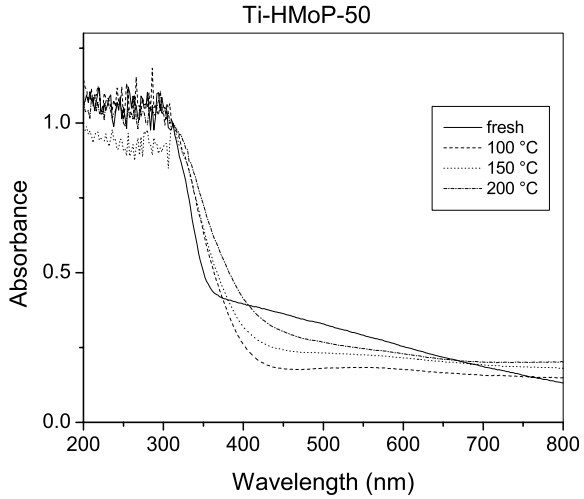

Fig. 5 UV-Vis spectra of Ti-HMoP-50 (measured at room temperature) as a function of annealing temperature.

Table 1. Band gap energy (measured at ambient temperature) as a function of annealing temperature

Sample	Temperature (°C)	E_g(eV)
TIHWP 50	fresh	3.38
	100	3.39
	150	3.39
	200	3.05
TIHMoP 50	fresh	3.20
	100	2.95
	150	2.88
	200	2.72

$$\alpha\,(h\nu) = A\left(h\nu - E_g\right)^{m/2}$$

where $\alpha(h\nu)$ is the absorption coefficient of the photon with energy $h\nu$, E_g the band gap, and m a coefficient that is 1 for a direct transition and 4 for an indirect transition [18]. From the spectrum a straight line is extrapolated to zero absorbance where $E_g = h\nu$.

The band gap varies from 3.38 eV for the HWP fresh sample (spectra not shown) to 3.05 eV for the same sample annealed at 200°C (Table 1). In the case of HMoP, the band gap varies from 3.2 to 2.72 eV in the same temperature range (Table 1). These band gap values are typical of those observed for sol-gel TiO_2. The thermal treatment favors a decrease in the band gap energy with increasing temperature.

3.4. TGA and EPR measurements

In Fig. 6, the TGA curve for the Ti–HMoP–50 sample shows that a weight loss of 25% occurs when the sample is annealed from 70°C (fresh sample) to 200°C. This weight loss is due to water desorption and dehydroxylation processes occurring in the sample, leading to oxygen vacancies. During this process,

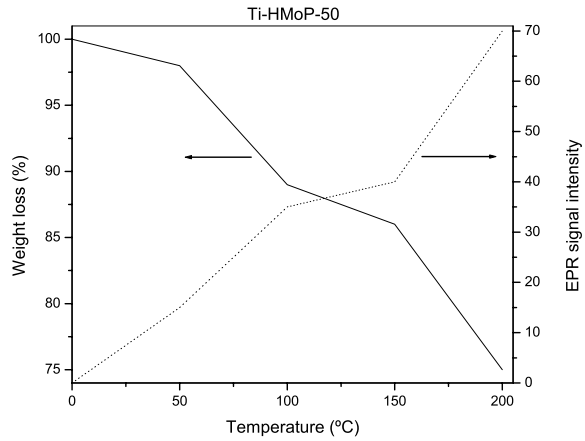

Fig. 6 Weight loss and EPR signal intensity of Ti-HMoP-50 as a function of annealing temperature.

a net magnetic moment can be measured by EPR in the same sample (Fig. 6).

The intense EPR signal at $g = 1.998$ (0.003) increases as the annealing temperature increases, which is attributed to the formation of O^- species. Analogous results are obtained for the Ti-HWP-50 sample.

4. Discussion

The FT-IR spectra of Ti-HWP-50 and Ti-HMoP-50 exhibit well-defined bands. In particular, the bands due to the Keggin anion are still observed up to 200°C, indicative of an intact Keggin structure. This result was confirmed by Raman scattering, in spite of the poor resolution of the Raman spectra of the annealed Ti-HWP-50 and Ti-HMoP-50 samples. The Keggin anion has an absorption band at 1080 cm^{-1}, which is attributed to the P—O bond of the central PO_4 tetrahedra. Generally, the P—O stretching modes lead to one or two bands between 1050 and 1100 cm^{-1} [13]. This shift is due to a change in the anion symmetry, arising from the interaction between HPA and TiO_2. The small low−frequency shifts in these bands observed for both samples with respect to the pure acids are due to hydrogen bonding interactions with the Keggin anion. These interactions are mediated by residual water and hydroxyl groups in the sol-gel titania.

During the annealing process, water desorption associated with reactions between adjacent = Ti—OH species to form —Ti—O—Ti = are observed. This phenomenon, well known for pure TiO_2, leads to the formation of the oxygen vacancies and O^- species that are associated with an increase in the intensity of the strong EPR signal during annealing. The oxygen vacancies give rise to an ionic n-type semiconductor, as confirmed by the decreasing band gap with increasing annealing temperature in both samples.

5. Conclusion

Titania modified with heteropolyacids was obtained by the sol-gel method. The incorporation of HPAs in titania via sol-gel processing produces mixtures of amorphous titania and a poorly crystalline anatase phase. In all samples, the Keggin structure is stabilized. Contrary to the case of pure TiO_2, the presence of HPAs inhibits the formation of anatase. The band gap energy values indicate that HPAs-TiO_2 systems could be used as efficient photocatalysts for the elimination of pollutants in air and water.

References

1. T. López, J. Hernández-Ventura, R. Gómez, F. Tzompantzi, E. Sánchez, X. Bokhimi, and A. García, J. Mol. Catal. A: Chemical. **167**,(2001) 110.
2. A.J. Maira, K.L. Yeung, C.Y. Lee, P.L. Yue, and C.K. Chang, J. Catal. **192** (2000) 185.
3. D. Chen and A.K. Ray, Appl. Catal. B: Environ. **23** (1999) 143.
4. V. Brezova and J. Stasko, J. Catal. **147** (1994) 156.
5. D.S. Muggly, J.T. Mc Cue, and J.L. Falconer, J. Catal. **173** (1998) 470.
6. J.M. Hermann, Catal. Today **53** (1999) 115.
7. A. Sclafini and J.M. Hermann, Photochem. Photobiol. A: Chem. **113** (1998) 251.
8. R. Gómez, T. López, E. Ortiz-Islas, J. Navarrete, E. Sánchez, F. Tzompanztzi, and X. Bokhimi, J. Mol. Catal. A: Chem. 193 (2003) 217.
9. K. Na, T. Okuhara, and M. Misono, J. Catal. 170 (1997) 96.
10. T. Yamase, N. Takabayasi, and M. Kaji, J. Chem. Soc. Dalton Trans. (1984) 793.
11. R. Akid and J.R. Darwent, J. Chem. Soc. Dalton Trans. (1985) 395.
12. J.G. Hernández-Cortéz, T. López, M.E. Manriquez, R. Gómez, and J. Navarrete, J. Sol-Gel Sci. Technol. **26** (2003) 1.
13. C. Rocchiccioli-Deltcheff, M. Fournier, R. Franck, and R. Thouvenot, Inorg. Chem. **22** (1983) 207.
14. J.C. Edwards, C.Y. Thiel, B. Benac, and J.F. Knifton, Catal. Lett. **51** (1998) 77.
15. A. Larbot, I. Laaziz, J. Marignan, and J.F. Quinson, J. Non-Crystal. Solids **147–148** (1992) 157.
16. K. Nakamoto, Infrared and Raman Spectra of Inorganic and Coordination Compounds, 3rd edn., (John Wiley and sons, New York, 1977).
17. U. Balachandran and N.G. Eror, J. Solid State Chem. **42**, 276 (1982).
18. W.B. Hannay, *Treatise on Solid State Chemistry* (Plenum Press, New York,1976) Vol.3 ch. 3.